J Biol Inorg Chem (2009) 14:261–271
DOI 10.1007/s00775-008-0446-8

ORIGINAL PAPER

A quinazoline-derivative DOTA-type gallium(III) complex for targeting epidermal growth factor receptors: synthesis, characterisation and biological studies

Raquel Garcia · Petra Fousková · Lurdes Gano · António Paulo · Paula Campello · Éva Tóth · Isabel Santos

Received: 5 August 2008 / Accepted: 14 October 2008 / Published online: 13 November 2008

Abstract The novel DOTA-like chelator 1,4,7,10-tetraazacyclododecane-1-{4-[(3-chloro-4-fluorophenyl)amino] quinazoline-6-yl}propionamide-4,7,10-triacetic acid (H_3L) was synthesised by alkylation of 1,4,7,10-tetraazacyclododecane-1,4,7-tris(*t*-butyl acetate) with *N*-{4-[(3-chloro-4-fluorophenyl)amino]quinazoline-6-yl}-3-bromopropionamide, followed by hydrolysis of the ester groups with trifluoracetic acid. H_3L has been fully characterised by multinuclear NMR spectroscopy, mass spectrometry and high-performance liquid chromatography (HPLC). Five protonation constants, log K_{Hi}, of H_3L were determined by potentiometry and UV–vis spectrophotometry and the values found are 10.47, 9.18, 5.24, 4.00 and 2.23. These methods, complemented with variable-pH ^{71}Ga NMR studies, allowed us to ascertain the stability constant of the Ga(III) complex of L. GaL has a remarkably high thermodynamic stability constant (log $K_{ML} = 24.5$). The radioactive complex ^{67}GaL was prepared in high yield and high radiochemical purity. Its HPLC chromatogram is identical to that obtained for the GaL complex prepared at the macroscopic level. At pH 7.4, ^{67}GaL has an overall neutral charge, is highly hydrophilic (log $D = -1.02 \pm 0.03$) and presents high in vitro stability in physiological media and in the presence of an excess of diethylenetriaminepentaethanoic acid . In vitro studies indicated that H_3L and GaL do not inhibit the cell growth of epidermal growth factor receptor expressing cell lines, such as A431 cervical carcinoma cells, a result which agrees with the very low cell internalisation found for ^{67}GaL in the same cell line. Biodistribution studies in mice indicated high in vivo stability for ^{67}GaL, a high total excretion rate and a relatively slow blood clearance, in full accordance with its hydrophilic character and the relatively important protein binding.

Keywords Epidermal growth factor receptors · Tyrosine kinase inhibitors · DOTA derivatives · Gallium

Electronic supplementary material The online version of this article (doi:10.1007/s00775-008-0446-8) contains supplementary material, which is available to authorized users.

R. Garcia · L. Gano · A. Paulo · P. Campello · I. Santos (✉)
Unidade de Ciências Químicas e Radiofarmacêuticas,
Instituto Tecnológico e Nuclear,
Estrada Nacional 10, Apartado 21,
2686-953 Sacavém, Portugal
e-mail: isantos@itn.pt

P. Fousková · É. Tóth
Centre de Biophysique Moléculaire CNRS,
Rue Charles Sadron,
45071 Orléans Cedex 2, France

Introduction

The epidermal growth factor (EGF) receptor (EGFR) is a tyrosine kinase (TK) receptor which is overexpressed in a wide variety of solid tumours, being normally associated with poor prognosis [1]. The EGFR family includes four distinct, but structurally similar receptors: EGFR/ErbB-1, HER2/ErbB-2, HER3/ErbB-3 and HER4/ErbB-4. EGFR is a 170-KDa glycoprotein which contains an extracellular ligand-binding domain, a lipophilic transmembrane region and an intracellular protein TK domain [1–3]. Several ligands bind to and activate the EGFR, such as EGF, transforming growth factor-α, amphiregulin, heparin-binding EGF-like growth factor, betacellulin and neu differentiation factor, also termed "heregulin" [1]. Among these, EGF and transforming growth factor-α are the most

important endogenous stimulatory ones [4]. A better understanding of EGFR and its ligands has motivated extended research on new therapeutic strategies to target these receptors. Monoclonal antibodies directed against the extracellular receptor domain, and small molecules which interfere at the intracellular portion of the receptor, preventing TK phosphorylation and inhibiting activation of signal transduction pathways, have been the most explored pharmacological therapeutic strategies. [1, 5]. Several TK inhibitors have been explored, the most potent, selective and approved being gefitinib (Iressa®) and erlotinib (Tarceva®), which act as reversible ATP-competitive EGFR-TK inhibitors [4, 5]. Such quinazoline derivatives exhibit high affinity for the EGFR-associated TK (EGFR-TK), competing with and preventing binding of ATP to the intracellular TK domain. Gefitinib, a fluorine-containing anilinoquinazoline, has been approved for the treatment of patients with advanced non-small-cell lung cancer (NSCLC). Erlotinib has also been approved for use in patients with locally advanced or metastatic NSCLC [6]. Mutations of the EGFR gene have been identified in specimens from patients with NSCLC who have a response to the EGFR-TK inhibitors gefitinib and erlotinib. EGFR mutations such as EGFR T790M commonly lead to resistance to these agents, limiting their long-term efficacy. Irreversible EGFR inhibitors can overcome resistance and seem promising in this regard [7]. More recently, several attempts have been made to design PET probes for imaging EGFRs, based on quinazoline analogues [6–17]. We and others have also been involved in designing novel compounds potentially applicable for early single photon emission scintigraphy detection and staging of EGFR-positive tumours, based on a quinazoline moiety [6, 18, 19]. Given our interest in $^{67/68}$Ga for nuclear molecular imaging, we chose to synthesise and evaluate gallium complexes bearing a quinazoline moiety. Herein, we report the synthesis and characterisation of a DOTA-like chelator bearing a quinazoline moiety, as well as the synthesis, characterisation and biological evaluation of the corresponding gallium complex.

Materials and methods

Materials and instruments

All chemicals and solvents were of reagent grade and were used without purification unless stated otherwise. NMR (^{1}H, ^{13}C, ^{19}F, ^{1}H–^{1}H correlation spectroscopy, heteronuclear single quantum coherence and heteronuclear multiple bond correlation) data were obtained using a Varian Unity 300-MHz spectrometer. ^{1}H and ^{13}C chemical shifts are reported in parts per million and were referenced relative to the residual solvent signals or to tetramethylsilane. ^{71}Ga NMR spectra were recorded using a Bruker Avance 500 (11.75-T, 152.5-MHz) spectrometer at 25 °C. The samples were measured in 10-mm NMR tubes. An insert tube with 9 mM $Ga(NO_3)_3$ in D_2O (p*D* 1.71) was used as an external reference and to lock the signal. The sample concentration was 1 mM and the gallium(III)-to-ligand ratio was 1:1.

The $Ga(NO_3)_3$ solution was prepared by dissolving 99.99% gallium metal in HNO_3 (the final pH was 1.3). The Ga^{3+} concentration was determined by adding excess Na_2H_2EDTA solution to the $Ga(NO_3)_3$ solution, and titrating back the Na_2H_2EDTA with Pb^{2+} at pH 5.8 in the presence of xylenol orange indicator.

IR spectra were recorded as KBr pellets with a Bruker Tensor 27 Fourier transform IR spectrometer. C, H, N analyses were performed using a CE Instruments EA 110 automatic analyser. Electrospray ionisation mass spectrometry (ESI-MS) was performed using an atmospheric pressure ionisation ion trap (PO03MS) and a Bruker HCT electrospray ionisation quadrupole ion trap mass spectrometer. 1,4,7,10-Tetraazacyclododecane-1,4,7-tris(*t*-butyl acetate) (DO3A^{t}Bu) and *N*-{4-[(3-chloro-4-fluorophenyl) amino]quinazoline-6-yl}-3-bromopropionamide (Br-quina) were prepared according to published methods [18, 20]. Gallium-67 citrate was purchased from Mallinckrodt Medical (The Netherlands). High-performance liquid chromatography (HPLC) analysis of 1,4,7,10-tetraazacyclododecane-1-{4-[(3-chloro-4-fluorophenyl)amino]quinazoline-6-yl}propionamide-4,7,10-triacetic acid (H_3L), GaL and ^{67}GaL was performed with a PerkinElmer liquid chromatography (LC) pump 200 coupled to an LC 290 tunable UV–vis detector and to a Berthold LB-507A radiometric detector. Analysis and purification were achieved on Nucleosil columns (10 µm, 250 mm × 4 mm and 7 µm, 250 mm × 8 mm) using flow rates of 1 and 2 mL min^{-1}, respectively; UV detection was at 254 nm. For H_3L, eluent A was aqueous 0.05% CF_3COOH solution and eluent B was acetonitrile with 0.05% CF_3COOH. The gradient was as follows: 0–1 min, 85% eluent A, 15% eluent B; 1–36 min, 15–100% eluent B; 36–43 min, 100% eluent B; 43–45 min, 0–85% eluent A; 45–50 min, 85% eluent A, 15% eluent B. For GaL and ^{67}GaL, eluent A was aqueous NEt_3/CH_3COOH [2.1:2.8 (v/v)] solution and eluent B was acetonitrile. The gradient was as follows: 0–15 min, 80% eluent A, 20% eluent B; 15–25 min, 20–30% eluent B; 25–45 min, 70% eluent A, 30% eluent B. Labelling efficiency was assessed using ascending silica gel thin-layer chromatography (ITLC-SG) strips (Polygram, Macherey Nagel) developed with the mobile phase 0.9% NaCl /CH_3COOH [9:1 (v/v)]. The radioactive distribution on the thin-layer chromatography strips was detected using a Berthold LB 505 detector coupled to a radiochromatogram scanner. The ^{67}GaL migrates with

$R_t = 0.7$, while ionic gallium-67 citrate migrates with $R_t = 1$. Colloidal radioactive species, if formed, remain at the origin.

Synthesis of 1,4,7,10-tetraazacyclododecane-4,7,10-tricarboxymethyl-*tert*-butylester-1-{2-[4-(3-chlorofluorophenyl)amino]quinazoline-6-yl}propionamide

A solution of DO3A^{t}Bu (120 mg, 0.20 mmol), Br-quina [18] (113 mg, 0.29 mmol) and K_2CO_3 (122 mg, 0.88 mmol) in 20 mL of dried acetonitrile was heated at 65 °C for 48 h. After this time, the mixture was filtered and the supernatant dried under vacuum. The solid obtained was used without further purification for the synthesis of H_3L.

For characterisation, 1,4,7,10-tetraazacyclododecane-4,7,10-tricarboxymethyl-*tert*-butylester-1-{2-[4-(3-chlorofluorophenyl)amino]quinazoline-6-yl}propionamide (DO3A^{t}Bu-quina) was purified by silica gel column chromatography [MeOH/AcOEt/NH_4OH (25%) (1:8:0.2) (v/v/v) to MeOH/NH_4OH (25%) (9:0.2) (v/v)]. Removal of the solvent from the collected fractions yielded DO3A^{t}Bu-quina as a yellow solid. ^{1}H NMR [300 MHz, $CDCl_3$, δ (ppm)]: 10.64 (s, CONH, 1H), 8.72 [d, CH, H(5), 1H], 8.57 [s, CH, H(2), 1H], 8.23–8.26 [m, CH, H(2′), H(7), 2H], 7.82–7.77 [m, CH, H(6′), 1H], 7.52 [d, CH, H(8), 1H], 7.05 [t, CH, H(5′), 1H], 6.40 (br, NH, 1H), 6.10 (br, NH, 1H), 3.38–2.18 (m, CH_2N, CH_2COO^tBu, 26H), 1.99 (s, CH_3, 9H), 1.45 (s, CH_3, 9H), 1.39 (s, CH_3, 9H).^{13}C NMR [$CDCl_3$, δ (ppm)]: 175.4, 172.7, 172.3, 171.9, 157.7, 153.0, 145.4, 138.1, 136.0, 127.2, 126.8, 123.9, 122.0, 120.1, 116.1, 115.3, 111.4, 82.1, 82.0, 82.0, 56.1, 55.4, 52.4–48.1, 47.2, 32.9, 28.0, 27.9, 27.7.

Synthesis of H_3L

DO3A^{t}Bu-quina was dissolved in 1 mL of trifluoroacetic acid. The reaction mixture was stirred overnight at room temperature. Trifluoroacetic acid was removed in a vacuum, and the residue was washed repeatedly with ethanol (4 × 2 mL) and dried, to remove residual trifluoroacetic acid. The product was purified by reversed-phase HPLC (RP-HPLC). After evaporation of the eluent, H_3L was obtained as pale-yellow solid (40 mg, overall yield 49%). ^{1}H NMR [300 MHz, D_2O, pH 2.94, δ (ppm)]: 8.42 [s, CH, H(2), 1H], 8.35 [s, CH, H(5), 1H], 7.78 [d, CH, H(8), 1H], 7.61 [dd, CH, H(7), 1H], 7.53 [dd, CH, H(2′), 1H], 7.27 [m, CH, H(6′), 1H], 7.11 [t, CH, H(5′), 1H], 3.59–2.73 (m, CH_2N, CH_2COOH, CH_2, 26H). ^{1}H NMR [300 MHz, D_2O, pH 9.15, δ (ppm)]: 7.89 [s, CH, H(2), 1H], 7.63 [s, CH, H(5), 1H], 7.42–7.21 [m, H(7), H(2′), H(8), CH, 3H], 7.01 [m, H(6′), CH, 1H], 6.91 [t, H(5′), CH, 1H], 3.50–3.27 (m, CH_2COOH, 6H), 3.11–2.81 (m, CH_2N, CH_2, 18H), 2.44 (m, CH_2, 2H). ^{13}C NMR [CD_3CN, δ (ppm)]: 174.0 (COOH), 171.9 (CONH), 169.9 (COOH), 161.5, 157.8, 150.6, 140.4, 136.2, 134.9, 130.2, 128.8, 126.4, 121.8, 121.5, 117.8, 113.6, 55.7, 54.9, 52.0, 51.4, 50.8, 50.5, 30.7, 22.0. IR (cm^{-1}, KBr pellet): 1,672.5 (s, $\nu_{C=O}$), 3,490 (b, ν_{O-H}). ESI-MS(+) *m/z* (relative intensity): 728 [M + K]$^+$, 711 [M + Na]$^+$, 689 [M]$^+$, 345 [M]$^{2+}$. Retention time 9.75 min. Anal. Calcd. for $C_{31}H_{38}N_8O_7FCl{\cdot}4CF_3COOH$: C, 40.90; H, 3.70; N, 9.78. Found: C 39.69; H, 2.98; N, 9.95.

Potentiometric and UV–vis studies of H_3L and its gallium(III) complex

To determine the ligand protonation constants and the stability constant of GaL, potentiometric titrations were carried out in a cell thermostated at 25 °C, at an ionic strength I(KCl) = 0.1 M and in the presence of extra HCl or KOH in the –log [H$^+$] range 3–12, using a combined glass electrode (LL Biotrode, Metrohm) connected to a Metrohm 827 pH/ion meter, equipped with a Metrohm Dosimat 765 automatic burette. The initial volume was 3 mL, the concentration of the ligand was 0.001 or 0.002 M and the gallium(III)-to-ligand ratio was 1:2. An inert atmosphere was ensured by constant passage of N_2 through the solution. The H$^+$ concentration was obtained from the measured pH values, according to the method proposed by Irving et al. [21]. The protonation and stability constants were calculated with the program PSEQUAD [22]. The errors given correspond to one standard deviation. The protonation constants β_n are defined by $\beta_n = [H_nL]/([H]^n \times [L])$; therefore, $\log K_{H1} = \log \beta_1$, $\log K_{H2} = \log \beta_2 - \log \beta_1$, etc. The stability constant is defined by $\beta_{pqr} = [M_pH_qL_r]/([M]^p \times [H]^q \times [L]^r)$.

The protonation constants of the ligand and of the GaL complex were also assessed by UV–vis measurements, carried out using a PerkinElmer Lambda 19 spectrometer in the region from 200 to 400 nm with data steps of 1 nm. The sample concentrations were approximately 10 μM and a constant temperature of 25 °C was maintained by using thermostatable cells with 1-cm optical length.

Preparation of ^{67}GaL

A volume of 300 μL (1.85–33.3 MBq/50–900 μCi) of gallium-67 citrate and 100 μL of a 0.02 M aqueous solution of H_3L were placed in a 5-mL glass vial and the pH was adjusted to approximately 6. The vial was then heated at 100 °C for 15 min, cooled to room temperature and the final solution was analysed by HPLC. To investigate the presence of possible hydrolysed gallium(III) species, ITLC-SG was performed. HPLC: $R_t = 16.3$ min; ITLC-SG: $R_f = 0.7$.

Synthesis of GaL

To a solution of H_3L in water (30 mg, 0.026 mmol) was added $Ga(NO_3)_3 \cdot 10H_2O$ (34 mg, 0.078 mmol). The pH was adjusted to 4 using an aqueous solution of NaOH. The resulting mixture was heated for 1 h at 95 °C and cooled to room temperature. After evaporation of the solvent under vacuum, GaL was obtained as a yellow solid [Yield: 40.2% (8 mg)]. ^{1}H NMR [300 MHz, D_2O, pH 7.81, δ (ppm)]: 7.95–7.91 (m, CH, 2H), 7.40–7.25 (m, CH, 3H), 7.15–6.93 (m, CH, 2H), 3.91 (t, CH_2, 2H), 3.39–3.02 (m, CH_2N, 22H), 2.68 (t, CH_2, 2H). ^{13}C NMR [CD_3CN, δ (ppm)]: 161.9, 161.3, 159.8, 155.4, 150.4, 147.5, 135.3, 133.1, 133.0, 126.6, 126.6, 126.0, 122.7, 121.0, 117.4, 103.6, 103.4, 58.9, 57.1, 55.7, 54.7, 53.9, 46.7, 33.7, 31.8. IR (cm^{-1}, KBr pellet): 1,644 (s, $\nu_{C=O}$), 1,681 (s, $\nu_{C=O}$), 3,449 (b, ν_{O-H}), 1,385 (s, ν_{C-N}). ESI-MS(+) *m/z* (relative intensity): 796 $[M + K]^+$, 779 $[M + Na]^+$, 757 $[M]^+$, 379 $[M]^{2+}$. HPLC $R_t = 16.0$ min.

Overall charge of ^{67}GaL

The overall charge of ^{67}GaL was determined by electrophoresis, using paper strips (Whatman no. 1, 3 MM) and tris(hydroxymethyl)aminomethane hydrochloride as a buffer (0.1 M, pH 7.4). A constant voltage of 250 V was applied for 1 h. The radioactive distribution on the strips was analysed using a Berthold LB 505 detector coupled to a radiochromatogram scanner.

Octanol–water partition coefficient of ^{67}GaL

The log $P_{o/w}$ value of ^{67}GaL, under physiological conditions (*n*-octanol/0.1 M phosphate-buffered saline, PBS, pH 7.4), was determined by the multiple back extraction method [23].

Transchelation with DTPA

The kinetic inertness of the radioactive complex ^{67}GaL was studied by measuring the rate of exchange of ^{67}Ga in the presence of 10^3 molar excess of diethylenetriaminepentaethanoic acid (DTPA), at pH 6 and at 37 °C. At different times (1, 4, 24, 120 h) aliquots were taken and analysed by HPLC, using the gradient described earlier.

In vitro plasma stability and plasmatic protein binding

A volume of 100 μL of ^{67}GaL was added to 1 mL of fresh human serum and incubated at 37 °C. After incubation (0, 0.5, 1, 2, 4, 24 and 96 h), aliquots were taken and the serum proteins were precipitated with 1 mL of ethanol. The serum was centrifuged at 3,500 rpm for 15 min at 4 °C and the supernatant (protein-free serum) was analysed by HPLC. The pellet was washed twice with 1 mL of PBS, followed by centrifugation at 3,000 rpm for 15 min. The activity in the sediment was compared with the activity in the supernatant, to estimate the percentage of complex bound to proteins.

In vitro evaluation

Cell line studies

The EGFR-expressing cell lines, A431 cervical carcinoma cells, kindly provided by J. Pirmettis and M. Paravatou (Demokritos Center, Greece), were maintained in Dulbecco's modified Eagle's medium containing Glutamax I and supplemented with 10% fetal bovine serum and 1% penicillin/streptomycin (Gibco, Invitrogen, UK), 100 IU per 100 μg mL^{-1}, in a 5% humidified CO_2 atmosphere at 37 °C. Cells were subcultured every 2 or 3 days.

In vitro cellular uptake studies

Uptake studies were performed with the A431 cell line. Cells were plated at a density of 2.5×10^5 cells per 0.5 mL per well of a 24-well plate in culture medium and allowed to attach overnight. After 24 h the medium was removed and replaced by fresh medium containing approximately 4×10^5 cpm per 0.5 mL of ^{67}GaL. After 0.25-, 0.5-, 1-, 2-, 3- and 5-h incubation periods, the cells were washed twice with cold PBS, lysed with a 0.1 M NaOH solution and the cellular extracts were counted for radioactivity. Each experiment was performed in quadruplicate.

In vitro growth inhibition assay

The A431 cells were seeded in a 96-well plate at a density of 10,000 cells per 200 μL per well and incubated for 24 h for attachment. The day after seeding, exponentially growing cells were incubated with various concentrations of H_3L or GaL (ranging from 1 nM to 100 μM in four replicates) for 24 h. Controls consisted of wells without drugs. The medium was removed and the cells were incubated for 3 h in the presence of 0.5 mg mL^{-1} 3-(4, 5-dimethylthiazol-2-yl)-2,5-diphenyltetrazolium bromide (MTT; Sigma) in PBS (Gibco, Invitrogen, UK) at 37 °C. The MTT solution was removed and 200 mL per well of dimethyl sulfoxide was added. After thorough mixing, the absorbance of the wells was read in an ELISA reader at test and reference wavelengths of 540 and 620 nm, respectively. The mean of the optical density of different replicates of the same sample and the percentage of each value was calculated (the mean of the optical density of

various replicates divided by the optical density of the control). The percentage of the optical density was plotted against drug concentration on a semilog chart and the IC_{50} from the dose response curve was determined.

Biodistribution studies

The in vivo behaviour of ^{67}GaL was evaluated in groups of four female CD-1 mice (randomly bred, Charles River) weighing approximately 20–25 g each. A volume of 100 μL of the preparation (0.37–2.85 MBq/10–77 μCi) was intravenously injected into the mice via the tail vein and the mice were maintained on a normal diet ad libitum. Mice were killed by cervical dislocation at 0.25, 1, 4, and 24 h after injection. The injected radioactive dose and the radioactivity remaining in the mouse after it had been killed were measured with a dose calibrator (Aloka, Curiemeter IGC-3, Tokyo, Japan). The difference between the radioactivity in the injected and the killed mouse was assumed to be due to total excretion from whole-body mouse. Blood samples were taken by cardiac puncture at the time the mouse was killed. Tissue samples of the main organs were then removed, weighed and counted in a gamma counter (Berthold). Biodistribution results were expressed as a percentage of the injected dose (% ID) per organ and/or per gram of tissue. For blood, bone and muscle, total activity was calculated assuming that these organs constitute 6, 10 and 40% of the total weight, respectively. The remaining activity in the carcass was also measured with a dose calibrator.

The experiments were conducted in compliance with the national law and with the EU Guidelines for Animal Care and Ethics for animal experiments.

Results and discussion

Synthesis and characterisation of H_3L

As indicated in Scheme 1, the novel bifunctional ligand H_3L was synthesised in two steps. In the first step, DO3A^{t}Bu was alkylated with the bromide quinazoline derivative Br-quina [18], in the presence of potassium carbonate. Then, the *tert*-butyl protecting groups in DO3A^{t}Bu-quina were removed with trifluoroacetic acid. After HPLC purification, H_3L was obtained in a pure form and with an overall yield of 49%. The bifunctional chelator H_3L was characterised by elemental analysis, ^{1}H and ^{13}C NMR, IR spectroscopy, RP-HPLC analysis and mass spectrometry.

At room temperature and in D_2O solution (pD ~3), the ^{1}H NMR spectra of H_3L show broad resonances associated with the macrocyclic moiety and the ethylenic spacer. Upon increasing the pH, the chemical shift and the shape of the resonances relative to those of the quinazoline moiety undergo limited changes. In contrast, the shape and the splitting of the resonances related to the macrocycle moiety and the linker change significantly with pH, reflecting the protonation of the nitrogen atoms and carboxylate groups of the tetraazamacrocycle. At pD 9.55 all the resonances could be assigned, with the pattern of the spectrum at this pD being in agreement with the formulation proposed for H_3L (see the electronic supplementary material).

Acid–base behaviour of H_3L

A potentiometric titration of the ligand was performed to determine its protonation constants. The five log K_{Hi}

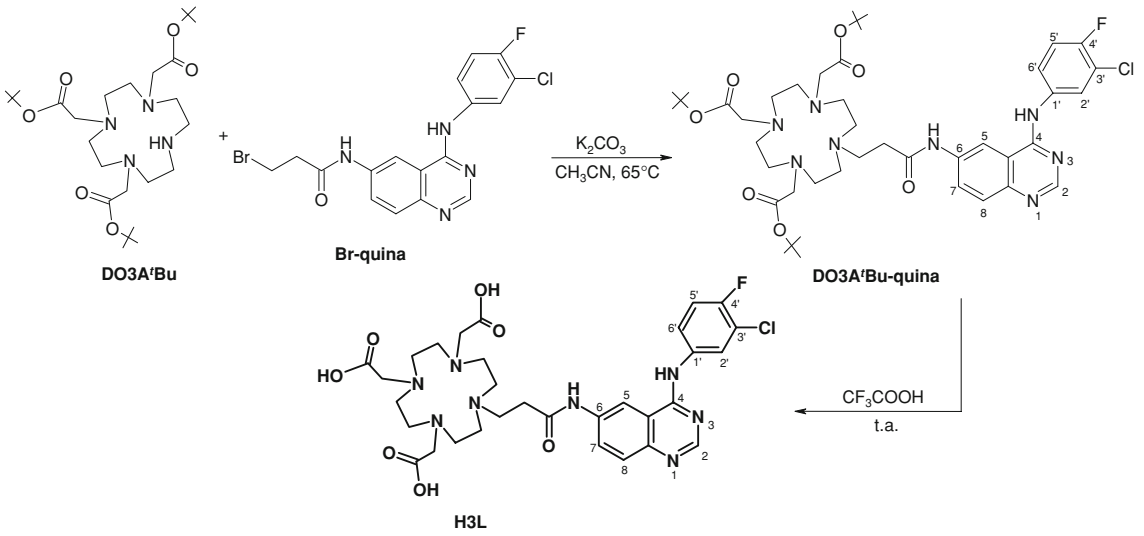

Scheme 1 Synthesis of H_3L

Table 1 Protonation constants of L^{3-} and $DOTA^{4-}$ (25 °C, I = 0.1 M)

Ligand	log K_{H1}	log K_{H2}	log K_{H3}	log K_{H4}	log K_{H5}
L	10.47 ± 0.02	9.18 ± 0.02	5.24 ± 0.03	4.00 ± 0.02	2.23 ± 0.04
DOTA [24]	11.14	9.69	4.85	3.95	–

values obtained are listed in Table 1 ($K_{Hi} = [H_iL]/[H_{i-1}L][H]$). Similar to H_4DOTA and related tetraazamacrocycles, the first two protonation constants can be assigned to the protonation of macrocyclic amines, while the last two protonation constants were attributed to the carboxylates. The third protonation constant (log K_{H3} = 5.24) was ascribed to the secondary amine of the pendant arm. This assignment was also supported by a UV–vis titration performed on the ligand between pH 2.8 and 7.6. The aromatic part of the ligand shows a strong absorption in the region from 200 to 400 nm. The intensity and the position of the absorption bands change upon varying the pH, owing to the protonation of the secondary amine (Fig. 1). The log K_H value calculated from this experiment was 5.21 ± 0.04, which corresponds well to log K_{H3} = 5.24 determined from the potentiometric titration.

Stability constant of the gallium(III) complex

The stability and the protonation constant of GaL were assessed in aqueous solution by using pH potentiometry, UV–vis spectrophotometry and ^{71}Ga NMR spectroscopy. To circumvent the slow formation of GaL in the acidic pH region, and to avoid the formation of the insoluble $Ga(OH)_3$, which can be present in gallium(III) solutions at relatively low pH (approximately 3–4), the GaL system was titrated with an HCl solution from an initial pH of 12. At this high pH, the ligand is completely deprotonated and gallium(III) is present in the form of soluble $[Ga(OH)_4]^-$.

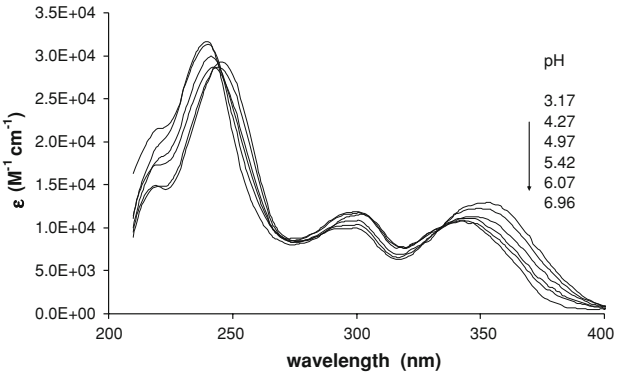

Fig. 1 Representative UV–vis spectra of 16 μM 1,4,7,10-tetraazacyclododecane-1-{4-[(3-chloro-4-fluorophenyl)amino]quinazoline-6-yl}propionamide-4,7,10-triacetic acid (H_3L) as a function of pH; 25 °C, I = 0.1 M (KCl)

Upon decreasing the pH, GaL forms without the formation of the insoluble $Ga(OH)_3$. On the other hand, the complex formation is also expected to be fast in the basic pH region. To further prevent the formation of $Ga(OH)_3$ precipitate, we used a 1:2 $[Ga(OH)_4]^-$-to-L ratio. Moreover, the titration was performed slowly, by addition of very small quantities of HCl (2 μL of 0.054 M HCl), and vigorous stirring of the solution, which should limit the local pH decrease after each HCl addition. Under these conditions, the pH was stabilised within a few minutes in the pH range 12–8, which was then used for the calculation of the stability constant. From this potentiometric titration, a stability constant of log K_{GaL} = 24.5 ± 0.5 was estimated. In the calculations, we used the following hydrolysis constants for Ga^{3+}: log $\beta_{Ga(OH)} = -2.9$, log $\beta_{Ga(OH)_2} = -6.0$, log $\beta_{Ga(OH)_3} = -11.0$, and log $\beta_{Ga(OH)_4} = -17.3$ ($\beta_{Ga(OH)_i} = [Ga(OH)_i]/[Ga^{3+}][OH]^i$) [25]. To determine the protonation constant of the GaL complex, log K_{HGaL}, we performed a titration by UV–vis spectrophotometry. Equivalent amounts of the ligand and $[Ga(OH)_4]^-$ were mixed at pH 12, then the pH was adjusted with diluted HCl. In the region from 220 to 400 nm, the spectral changes occur between pH 3 and 5.5 and correspond to the protonation of the amine nitrogen on the noncoordinated aromatic pendant arm which does not participate in the complex formation (see the electronic supplementary material). The pH-dependent spectra allowed us to calculate a protonation constant of log K_{HGaL} = 4.25 ± 0.05. Table 2 gives the stability and protonation constants, as well as pM values for GaL and for other gallium complexes with related macrocycles.

To further confirm the stability constant of the GaL complex, ^{71}Ga NMR measurements were performed. In the ^{71}Ga NMR spectra, only Ga^{3+} in very symmetrical environments can be observed (such as $[Ga(H_2O)_6]^{3+}$ or $[Ga(OH)_4]^-$), while the NMR signals are extremely broad with biologically interesting ligands [27, 28]. We monitored the decrease of the $[Ga(OH)_4]^-$ peak at 1 mM overall gallium concentration and 1:1 Ga^{3+}-to-L ratio upon decreasing the pH from 10 to 8, a pH range which corresponds to the formation of the GaL complex from $[Ga(OH)_4]^-$. The experimental conditions were identical to those used in the potentiometric titration (25 °C, I = 0.1 M), except that we used equimolar amounts of L and Ga^{3+} (1 mM). The spectra are depicted in Fig. 2. The decrease of the $[Ga(OH)_4]^-$ signal intensity on decreasing

Table 2 Stability and protonation constants and pM for GaL, and other related gallium(III) complexes (25 °C, I = 0.1 M) (K_{GaL} = [GaL]/[Ga][L]; K_{HGaL} = [HGaL]/[GaL][H]; pM = −log $[Ga]_{noncomplexed}$ at $c_{Ga} = c_L$ = 1 μM, pH 7.5)

Complex	GaL	GaDOTA [24, 26]	GaTRITA [24, 26]	GaTETA [24, 26]	GaNOTA [24, 26]
log K_{GaL}	24.5 ± 0.5	21.33	19.91	19.74	30.98
log K_{HGaL}	4.25 ± 0.05	4.00	3.66	3.65	–
pM	12.93	10.75	9.96	9.88	20.61

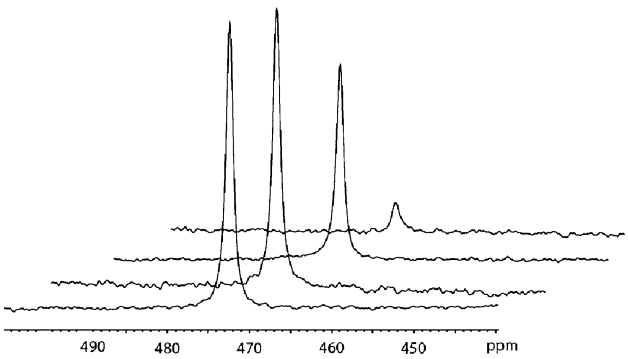

Fig. 2 Representative ^{71}Ga NMR spectra of a solution of Ga^{3+} and H_3L at pH values of 10.12, 9.65, 8.89 and 7.93 (from *front* to *back*), at 25 °C, I = 0.1 M (KCl). The only observable NMR signal corresponds to $[Ga(OH)_4]^-$. The spectra were referenced to $[Ga(H_2O)_6]^{3+}$ (pH 1.31, 250 ppm) contained in an inserted tube. The percentage of $[Ga(OH)_4]^-$ versus total Ga^{3+} in the sample is 100, 100, 60 and 6% (from *front* to *back*)

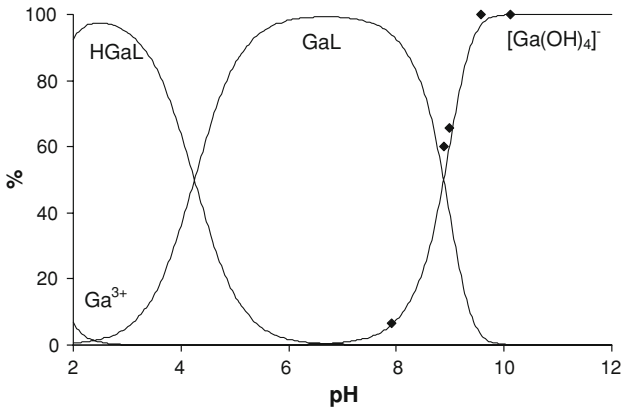

Fig. 3 Species distribution diagram of the GaL system. The experimental ^{71}Ga NMR data (*diamonds*) are plotted for pH values 10.12, 9.57, 8.98, 8.89 and 7.93

the pH demonstrates the formation of the GaL complex. To quantify the diminution of the $[Ga(OH)_4]^-$ signal, we used an insert containing a $Ga(NO_3)_3$ solution as an external reference. This allowed us to calculate a conditional stability constant for the GaL complex at each pH, which, by using the protonation constants of the ligand as determined above, was converted into a thermodynamic stability constant. The value calculated in this way is log K_{GaL} = 24.3, in perfect agreement with that obtained by potentiometry. The species distribution diagram calculated with this stability constant and the protonation constant of the complex obtained by spectrophotometry is depicted in Fig. 3. This figure also shows each individual experimental point measured in ^{71}Ga NMR. We should note that the potentiometric titration of the gallium(III)–ligand system starting from basic pH, complemented by ^{71}Ga NMR measurements, offers a convenient way to determine stability constants. Indeed, it circumvents the very slow complex formation in the acidic pH region and, depending on the stability of the complex, may avoid the formation of insoluble $Ga(OH)_3$.

On the basis of the thermodynamic stability constants and pM values, L is a better chelator for Ga^{3+} than 1,4,7,10-tetraazacyclododecane-1,4,7,10-tetraacetic acid (DOTA) or other related tetraazamacrocycles with a larger cavity size, such as 1,4,7,10-tetraazacyclotetradecane-1,4,8,11-tetraacetato (TETA) or 1,4,7,10-tetraazacyclotridecane-1,4,8,11-tetraacetic acid (TRITA) (Table 2) [24, 26]. However, the values found for GaL (log K_{GaL} = 24.5 and pM 12.9) are lower than the values previously described for GaNOTA (log K_{GaL} = 30.98 and pM 20.61). This evidences that Ga^{3+} fits better to the smaller cavity of 1,4,7-triazacyclononane-1,4,7-triacetic acid (NOTA), being six-coordinated by the three nitrogen atoms of the macrocycle backbone and by three oxygen atoms of the pendant carboxylate arms [29, 30]. However, we have to note that DOTA-type chelators are more advantageous for the labelling of biologically relevant molecules with $^{67/68}Ga^{3+}$ since they allow for an easy functionalisation via one of the carboxylate groups [29, 31]. In contrast, the modification of NOTA to yield a bifunctional chelator would involve a more complicated synthetic method, as the biomolecule has to be conjugated either through the methylenic carbons of the NOTA backbone or through a differentiated pendant arm, adequate to satisfy the octahedral coordination geometry of Ga^{3+} and the conjugation to a biomolecule [31]. The high thermodynamic stability constant of the Ga^{3+} complex with the modified DOTA and the easy conjugation of a biomolecule to a nitrogen atom of the backbone justifies why DOTA derivatives have been so widely used as bifunctional chelators for labelling different biomolecules with $^{67/68}$ Ga. Some relevant examples are ^{68}GaDOTATOC

(DOTA-D-Phe[1]-Tyr[3]-Octreotide), ^{68}GaDOTATATE (DOTA-Tyr[3]-Thr[8]-Octreotide) and ^{68}GaDOTANOC (DOTA-Nal[3]-Octreotide) explored for imaging of somatostatin receptors [32, 33]. Other promising target-specific radiotracers anchored on bifunctional DOTA are ^{68}GaDOTA–hEGF, ^{68}GaDOTA–albumin, ^{68}GaDOTA–thymidine analogue and ^{68}GaDOTA–bombesin [33–37].

Synthesis, characterisation and stability of ^{67}GaL

Labelling studies of H_3L were performed using gallium-67 citrate as the starting material, at pH 6 and 100 °C (Scheme 2). After 15-min reaction time, aliquots of the preparations were taken and analysed by RP-HPLC. The reaction is almost quantitative (radiochemical purity more than 97%) for final concentrations of the ligand (L) of 5×10^{-3} M. As exemplified in Fig. 4, the main radiochemical species formed appears at 16.3 min, and corresponds to ^{67}GaL. ^{67}GaL was obtained with a specific activity of approximately 24.2 MBq mg^{-1}, a value which compares well with what has been described for other ^{67}Ga complexes [32, 38, 39]. The chemical identity of ^{67}GaL was confirmed by comparison of its HPLC profile with that of the corresponding inactive gallium complex GaL, prepared at the macroscopic level. GaL was synthesised by reacting H_3L with 3 equiv of $Ga(NO_3)_3 \cdot 10H_2O$ at pH 4, and by heating the reaction mixture at 95 °C for 1 h (Scheme 2). GaL is a yellow solid and is moderately soluble in most common organic solvents and in water. Its characterisation involved IR spectroscopy, ^{1}H and ^{13}C NMR, HPLC analysis, and mass spectrometry. In the mass spectrum of GaL a prominent peak with the expected isotopic pattern was found at $m/z = 757$, which corresponds to the molecular ion $[M]^+$. The IR spectrum of GaL displays a broad band at 3,449 cm^{-1} attributed to ν_{O-H}, and

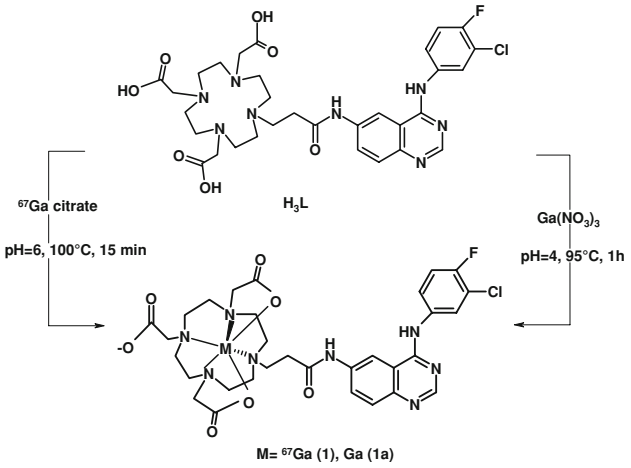

Scheme 2 Synthesis of GaL/^{67}GaL complexes

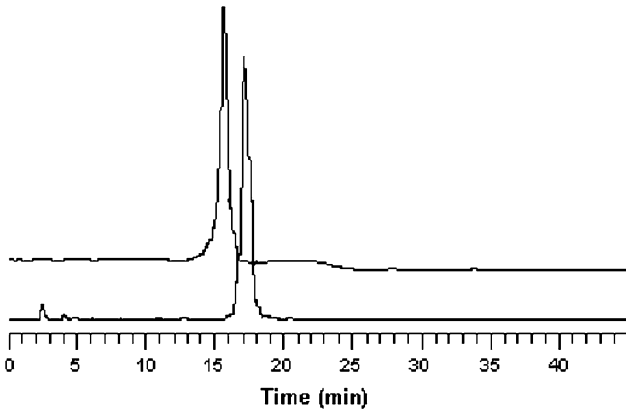

Fig. 4 Reversed-phase high-performance liquid chromatography (RP-HPLC) chromatogram of GaL (*top*) and ^{67}GaL (*bottom*)

two strong bands at 1,644 and at 1,681 cm^{-1} assigned to the coordinated and uncoordinated C=O of carboxylate groups, respectively.

As stated above, during the synthesis of gallium complexes some hydrolysed species can also be formed together with the main complex ^{67}GaL. If this is the case, these species cannot be identified by RP-HPLC, as they are retained in the column. To check for their presence, ^{67}GaL was analysed by ITLC-SG, using 0.9% NaCl/CH_3COOH [9:1(v/v)] as the eluent. In these conditions the hydrolysed species do not migrate ($R_t = 0$) and gallium-67 citrate migrates with $R_t = 1$. The ITLC-SG chromatogram of ^{67}GaL shows the presence of only one species corresponding to ^{67}GaL, with $R_t = 0.7$ (see the electronic supplementary material). This result, together with the RP-HPLC result, confirms that the experimental conditions chosen to prepare ^{67}GaL led to its almost quantitative formation (more than 97%).

The overall charge of ^{67}GaL, under physiological conditions, was evaluated by electrophoresis. For comparison, we also performed electrophoresis of gallium-67 citrate, which has a well-known and established negative charge [30]. The gallium-67 citrate migrates towards the anode, while ^{67}GaL does not migrate (see the electronic supplementary material). This behaviour does indicate that ^{67}GaL is neutral at physiological pH (7.4). These results are in full accordance with the protonation constant determined for GaL (log $K_{HGaL} = 4.25$) which predicts full deprotonation, and thus neutrality of the complex at physiological pH. Unfortunately, we did not get any single crystals to characterise GaL in the solid state. However, from a comparison with data in the literature for GaDOTA–D-PheNH$_2$ and Ga(DO3A-xy-TPP)$^+$ (DO3A-xy-TPP is triphenyl(4-((4,7,10-tris(carboxymethyl)-1,4,7,10-tetraazacyclododecan-1-yl)methyl)benzyl)phosphonium), the Ga^{3+} in GaL/^{67}GaL is expected to be hexacoordinated by the four nitrogen atoms of the macrocycle backbone and by

two oxygen atoms of two carboxylate pendant arms, displaying most probably a distorted octahedral coordination geometry [29–31]. This means that one carboxylate pendant arm in ^{67}GaL/GaL must be free, as previously found for other related gallium complexes. Therefore, the neutral overall charge found for ^{67}GaL under physiological conditions indicates that the free carboxylate of the noncoordinated pendant arm as well as the amine group in the quinazoline derivative are deprotonated. The presence of the free carboxylate group certainly justifies the high hydrophilic character found for ^{67}GaL/GaL under physiological conditions ($\log D = -1.02 \pm 0.03$). This feature has also been observed for other gallium(III) complexes anchored on DOTA-like chelators, which also present a deprotonated free carboxylate pendant arm [29–31].

For radiopharmaceutical applications, gallium complexes have to fulfil three requirements: to be resistant to hydrolysis, avoiding the formation of insoluble species such as [$Ga(OH)_3$], to bind reversibly to blood proteins and to be kinetically inert towards transchelation, as it affects the blood clearance and tissue distribution. For gallium(III), the most relevant plasmatic protein is transferrine, an iron-transport protein in blood with capability to bind Ga^{3+} with high affinity ($\log K_{GaL} = 20.3$) [30]. Having these requirements in mind and in order to predict in vivo results, we evaluated the in vitro stability of ^{67}GaL in saline and PBS solutions, in human serum and in the presence of an excess of DTPA, a chelator which has a stability constant with gallium(III) ($\log K_{GaL} = 25.1$) [24] higher than transferrine. We have found that ^{67}GaL is stable in saline and PBS solutions for up to 5 days at 37 °C, as no other soluble or insoluble species are formed. ^{67}GaL is also stable and kinetically inert in the presence of 10^3-fold excess of DTPA, as no degradation or transchelation of ^{67}GaL was found over a time interval of 5 days. Considering the stability constants of L, DTPA and transferrine with gallium(III), the kinetic inertness found for ^{67}GaL towards DTPA allows us to predict that in vivo ^{67}GaL will be kinetically inert towards transchelation with transferrine.

The stability of ^{67}GaL in serum as well as its binding to serum proteins was evaluated by incubating ^{67}GaL with fresh human serum (37 °C) at various time intervals. After precipitation of the proteic fraction, the radioactivity in the supernatant and in the precipitate was measured, and the supernatant was also analysed by RP-HPLC. The RP-HPLC analysis indicated that ^{67}GaL is stable for up to 6 days, as no other radiochemical species were detected (see the electronic supplementary material). A significant amount of radioactivity was in the proteic fraction, this amount being time-dependent: 22.1 and 51.3% of the total activity after 1 and 96 h of incubation, respectively. Taking into account the high stability constants and kinetic inertness of GaL, the relatively high values found in the proteic fraction most probably result from a reversible plasma protein binding of the intact complex, as observed for many other drugs. We can speculate that such binding must be due to the presence of a free carboxylate group at physiological pH [40].

Biological evaluation of ^{67}GaL

In vitro cellular uptake and inhibition studies

The degree of internalisation of ^{67}GaL in intact A431 cells is a very important parameter to obtain a first insight into the potential of our compound for application as a biomarker for EGFR-TK imaging. Internalisation studies were performed at room temperature and the degree of cellular uptake was evaluated at different time points. The percentage of cell binding was found to be very low (less than 0.2% at 5 h of incubation), indicating that no significant cell uptake and/or internalisation took place. The potential of H_3L and GaL to inhibit the growth of intact A431 cells was evaluated using the MTT assay. The results obtained

Table 3 Biodistribution data for ^{67}GaL in Charles River mice, at 15, 60, 4 and 24 h after injection (% ID g^{-1} ± standard deviation)

Organ	15 min	60 min	4 h	24 h
Blood	6.84 ± 0.65	4.21 ± 0.79	0.64 ± 0.55	0.04 ± 0.01
Heart	2.16 ± 0.36	1.40 ± 0.21	0.20 ± 0.04	0.06 ± 0.01
Liver	3.82 ± 0.28	3.00 ± 0.81	0.77 ± 0.53	0.40 ± 0.06
Spleen	1.37 ± 0.57	1.08 ± 0.16	0.72 ± 0.48	0.54 ± 0.04
Lung	4.72 ± 0.27	3.04 ± 0.26	0.58 ± 0.37	0.26 ± 0.04
Kidneys	6.22 ± 1.18	5.21 ± 0.44	1.44 ± 0.22	0.64 ± 0.08
Stomach	0.44 ± 0.10	1.34 ± 0.37	0.44 ± 0.22	0.11 ± 0.07
Intestine	1.02 ± 0.29	1.48 ± 0.14	2.47 ± 0.09	0.16 ± 0.04
Muscle	0.94 ± 0.26	0.80 ± 0.09	0.04 ± 0.03	0.04 ± 0.01
Brain	0.19 ± 0.03	–	0.04 ± 0.02	0.01 ± 0.004
Pancreas	–	0.84 ± 0.12	0.04 ± 0.02	–
Excretion (% ID)	28.6 ± 5.7	52.3 ± 1.4	84.18 ± 1.89	95.55 ± 0.37

ID injected dose

show no inhibition of cell growth, for concentrations in the range from 1 nM to 100 μM. This result agrees with the very low internalisation found for ^{67}GaL in the same cell line.

Biodistribution and in vivo stability studies

Tissue distribution studies of ^{67}GaL were carried out in healthy female CD-1 mice to evaluate the in vivo stability and pharmacokinetic profile of the compound. Table 3 shows the biodistribution of ^{67}GaL for the most relevant organs as a function of time.

The most striking feature in the in vivo behaviour of ^{67}GaL is the high rate of total radioactivity excretion from the whole animal (28.6, 52.3, 84.2 and 95.6% of the injected dose 0.25, 1, 4 and 24 h after administration, respectively). Furthermore, the compound has a relatively slow clearance from the bloodstream (6.8 and 4.2% of ID g^{-1} 15 min and 1 h after administration, respectively). Consequently, some radioactivity localisation was found in highly irrigated organs such as liver, lungs and heart at early time points. At latter times (4 h after injection), there is no significant radioactivity retention in any particular major organ, except those involved in the excretory pathways (kidney and intestines). This fairly slow washout from organs such as blood, lungs and heart that clear over time is in agreement with the plasmatic protein binding found by in vitro assay. The high rate of total radioactivity excretion, combined with the relative high kidney uptake at 15 min (6.2 ± 1.2% of ID g^{-1}), which clears out with time, indicates that the main excretory route is the urinary tract, although with a small fraction eliminated via the hepatobiliary system. This pattern of excretion reflects the high hydrophilic character of the complex. The biodistribution profile of ^{67}GaL also indicates that no free ^{67}Ga is released from the complex, as Ga^{3+} would tend to localise significantly in liver and lungs owing to the strong binding capability to transferrine [29]. Further evidence of the high in vivo stability was obtained from the RP-HPLC analysis of urine samples collected at 4 h after injection, which proved that ^{67}GaL is excreted without any degradation (Fig. 5).

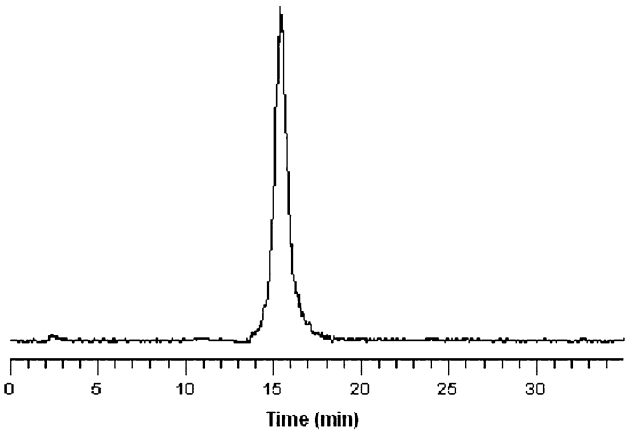

Fig. 5 RP-HPLC of the urine of a mouse injected with ^{67}GaL, 4 h after injection

Concluding remarks

A new DOTA-like bifunctional chelator bearing a quinazoline moiety, H_3L, was synthesised and fully characterised by multinuclear NMR spectroscopy, elemental analysis, ESI-MS and HPLC. The protonation constants for H_3L were determined by potentiometry and UV–vis titration ($\log K_{H1} = 10.47 \pm 0.02$, $\log K_{H2} = 9.18 \pm 0.02$, $\log K_{H3} = 5.24 \pm 0.03$, $\log K_{H4} = 4.00 \pm 0.02$, $\log K_{H5} = 2.23 \pm 0.04$). The stability constant of GaL was also determined by potentiometry and ^{71}Ga NMR. The high thermodynamic stability found ($\log K_{GaL} = 24.5 \pm 0.5$, pM 12.93) indicates that H_3L displays excellent affinity for Ga^{3+}, when compared with other 12-membered as well as 13- or 14-membered tetraazamacrocycles. This justifies the formation of ^{67}GaL in high yield and high radiochemical purity, its resistance to hydrolysis, and stability in physiological media. Moreover, ^{67}GaL forms relatively rapidly and is kinetically inert to transchelation in the presence of an excess of DTPA. ^{67}GaL is highly hydrophilic ($\log D = -1.02 \pm 0.03$) under physiological conditions, which certainly explains the very low A431 cell uptake. The inability to penetrate into the cells can also account for the absence of any in vitro growth inhibition of the A431 cells. ^{67}GaL shows a high in vivo stability; no Ga^{3+} is released from the complex, as confirmed by its biological profile and RP-HPLC analysis of the urine of mice into which ^{67}GaL was injected. The most striking feature of the pharmacokinetics of ^{67}GaL is the high rate of total excretion (84.2%, 4 h after injection), in spite of a relatively slow blood clearance (0.64% ID g^{-1}, 4 h after injection), certainly owing to the high hydrophilicity of the complex and to its binding to the proteic fraction, respectively. Despite the favourable biodistribution profile in healthy animals, in vivo studies in tumour-bearing mice were not performed owing to the low uptake of ^{67}GaL in A431 cells, which led us to expect a low in vivo retention in target tumour tissues. The inability to penetrate the cell membrane indicates that ^{67}GaL is not adequate for EGFR-TK imaging. Taking into account the whole set of results, further work must be done to promote the penetration of the cell membrane and to optimise the biological performance of DOTA-like gallium complexes bearing a quinazoline pharmacophore. This optimisation involves maintaining the DOTA-like backbone and

introducing structural modifications in the bifunctional chelator and/or linker to increase the lipophilicity of the gallium complex, an essential requirement to improve cell penetration and tissue permeability.

Acknowledgments This work was partially support by the FCT (POCTI/QUI/57632/2004) and by COST Action D38. R.G. would like to thank the Fundação para a Ciência e Tecnologia for a post-doctoral research grant. We wish to acknowledge Ana Coelho and Joaquim Marçalo from the Laboratório de Espectrometria de Massa at the ITQB-Universidade Nova de Lisboa, Oeiras, Portugal, and from the ITN, Sacavém, Portugal, respectively, for the ESI-MS analysis. We thank Zsolt Baranyai for his help in preparing the $Ga(NO_3)_3$ solution. The quadrupole ion trap mass spectrometer was acquired with the support of the Programa Nacional de Reequipamento Científico (contract REDE/15037/REM/2005-ITN) of Fundação para a Ciência e a Tecnologia and is part of RNEM-Rede Nacional de Espectrometria de Massa.

References

1. Herbst RS (2004) Int J Radiat Oncol Biol Phys 59(2):21–26
2. Wong RWC, Guillaud L (2004) Cytokine Growth Factor Rev 5:147–156
3. Mendelsohn J, Baselga J (2003) J Clin Oncol 21(14):2787–2799
4. Sridhar SS, Seymour L, Shepherd FA (2003) Lancet Oncol 4(7):397–406
5. Laskin JJ, Sandler AB (2004) Cancer Treat Rev 30:1–17
6. Cai W, Niu G, Chen X (2008) Eur J Nucl Med Mol Imaging 35:186–208
7. Yu Z, Boggon TJ, Kobayashi S, Jin C, Ma PC, Dowlati A, Kern JA, Tenen DG, Halmos B (2007) Cancer Res 67(21):10417–10427
8. Bonasera TA, Ortu G, Rozen Y, Krais R, Freedman NM, Chisin R, Gazit A, Levitzki A, Mishani E (2001) Nucl Med Biol 28:359–374
9. Dissoki S, Laky D, Mishani E (2006) J Labelled Comp Radiopharm 49:533–543
10. Johnström P, Fredriksson A, Thorell J-O, Stone-Elander S (1998) J. Labelled Comp Radiopharm 41:623–629
11. Ben-David I, Rozen Y, Ortu G, Mishani E (2003) Appl Radiat Isot 58:209–217
12. Mishani E, Abourbeh G, Rozen Y, Jacobson O, Laky D, Ben DI, Levitzki A, Shaul M (2004) Nucl Med Biol 31:469–476
13. Mishani E, Abourbeh G, Rozen Y, Jacobson O, Dissoki S, Daniel RB, Rozen Y, Shaul M, Levitzki A (2005) J Med Chem 48:5337–5348
14. Ortu G, Ben-David B, Rozen Y, Freedman NMT, Chisin R, Levitski A, Mishani E (2002) Int J Cancer 101:360–370
15. Shaul M, Abourbeh G, Jacobson O, Rozen Y, Laky D, Levitzki A, Mishani E (2004) Bioorg Med Chem 12:3421–3429
16. Mishani E, Abourbeh G (2007) Curr Top Med Chem 7:1755–1772
17. Breza N, Pató J, Orfi L, Hegymegi-Barakonyi B, Anhegyi PB, Varkondi E, Borbely G, Petak I, Keri G (2008) J Recept Signal Transduct 28(4):361–373
18. Fernandes C, Oliveira C, Gano L, Bourkoula A, Pirmettis I, Santos I (2007) Bioorg Med Chem 15(12):3974–3980
19. Fernandes C, Santos IC, Santos I, Pietzsch H-J, Kunstler J-U, Kraus W, Rey A, Margaritis N, Bourkoula A, Chiotellis A, Paravatou-Petsotas M, Pirmettis I (2008) Dalton Trans 3215–3225
20. Beeby A, Bushby LM, Maffeo D, Williams JAG (2002) J Chem Soc Dalton Trans 48–54
21. Irving HM, Miles MG, Pettit LD (1967) Anal Chim Acta 38:475
22. Zékány L, Nagypál I (1985) Computational methods for determination of formation constants. Plenum Press, New York, p 291
23. Troutner DE, Volkert WA, Hoffman TJ, Holmes RA (1984) Int J Appl Radiat Isot 35:467–470
24. Martell AE, Smith RM (2003) NIST standard reference database 46 (critically selected stability constants of metal complexes), version 7.0
25. Burgess J (1978) Metal ions in solution. Harwood, Chichester, p 314
26. Clarke ET, Martell AE (1991) Inorg Chim Acta 190:37–46
27. Glickson JD, Pitner TP, Webb J, Gams RA (1975) J Am Chem Soc 97:1679–1683
28. Akitt JW, Kettle D (1989) Magn Reson Chem 27:377–379
29. Liu S (2008) Adv Drug Deliv Rev 60:1347–1370
30. Bandoli G, Dolmella A, Tisato F, Porchia M, Refosco F (2008) Coord Chem Rev. doi:10.1016/j.ccr.2007.12.001
31. Léon-Rodríguez LM, Kovacs Z (2008) Bioconjug Chem 19(2):391–402
32. Heppeler A, Froidevaux S, Mäcke HR, Jermann E, Béhé M, Powell P, Hennig M (1999) Chem Eur J 5(7):1974–1981
33. Tanaka K, Fukase K (2008) Org Biomol Chem 6:815–828 and references therein
34. Velikyan I, Sundberg AL, Lindhe O, Höglund AU, Eriksson O, Werner E, Carlsson J, Bergström M, Långström B, Tolmachev V (2005) J Nucl Med 46:1881–1888
35. Schmid M, Neumaier B, Vogg ATJ, Wczasek K, Friesen C, Mottaghy FM, Buck AK, Reske SN (2006) Nucl Med Biol 33:359–366
36. Zhang H, Schuhmacher J, Waser B, Wild D, Eisenhut M, Reubi JC, Maecke HR (2007) Eur J Nucl Med Mol Imaging 34(8):1198–1208
37. Mier W, Hoffend J, Krämer S, Schuhmacher J, Hull WE, Eisenhut M, Haberkorn U (2005) Bioconjug Chem 16:237–240
38. Dadachova E, Park C, Eberly N, Ma D, Paik CH, Brechbiel MW (2001) Nucl Med Biol 28:695–701
39. Wang S, Lee RJ, Mathias CJ, Green MA, Low PS (1996) Bioconjug Chem 7:56–62
40. Goodman and Gillman's (1996) The pharmacological basis of therapeutics, 7th edn. McGraw-Hill, New York, p 12